
R-Block: Regularized block of Dropout for convolutional networks

Liqi Wang¹ Qiya Hu^{1*}

¹Academy of Mathematics and Systems Science, Chinese Academy of Sciences

Abstract

Dropout as a regularization technique is widely used in fully connected layers while is less effective in convolutional layers. Therefore more structured forms of dropout have been proposed to regularize convolutional networks. The disadvantage of these methods is that the randomness introduced causes inconsistency between training and inference. In this paper, we apply a mutual learning training strategy for convolutional layer regularization, namely R-Block, which forces two outputs of the generated difference maximizing sub models to be consistent with each other. Concretely, R-Block minimizes the losses between the output distributions of two sub models with different drop regions for each sample in the training dataset. We design two approaches to construct such sub models. Our experiments demonstrate that R-Block achieves better performance than other existing structured dropout variants. We also demonstrate that our approaches to construct sub models outperforms others.

1 Introduction

Convolutional Neural Networks (CNNs) are powerful tools in the field of computer vision. Regularization [1, 9, 11, 22, 25, 27, 14] is needed during CNN training to prevent overfitting and improve the generalization ability of the model. Among them, dropout [21] is a well-known regularization technique, which can perform implicit ensemble and reduce interdependence of neurons (co-adaptation) [14] by randomly dropping units in hidden layers during training. Although dropout works well in fully connected layers, it is nearly ineffective in convolutional layers where features are spatially correlated [6]. To address this dropout problem, many structured dropout methods have gradually been proposed [23, 18, 24, 12, 2, 10, 26, 16, 19, 3]. A drawback of these methods is that the randomly sampled sub models during training are different from the full model during inference [17, 29].

In this paper, we adopt a simple and effective strategy to regularize above inconsistency in CNNs, named as R-Block. Specifically, in each mini-batch training, the same sample goes through two sub models with completely different random drop regions and obtains the similar prediction outputs. R-Block minimizes the bidirectional losses between the two output distributions, that is, it adds deep mutual learning [28] of the two sub models with difference maximization, which can reduce the inconsistency between training and inference phases of model [15]. According to the structure of feature maps, we design two approaches to construct sub models with different drop regions.

From the perspective of convolutional neural network regularization, our proposed R-Block can be regarded as a new structured form of dropout. In our experiments, R-Block is much better than other

Funding: The work of the author was supported by the National Natural Science Foundation of China grant G12071469.

*Corresponding author.

existing structured dropout variants. Our results show that our approaches to construct sub models perform better than the alternatives.

Related Work. For CNNs with special structures, structured variants of dropout have been proposed such as SpatialDropout [23, 18], Max-pooling Dropout [24], DropBlock [6], Spectral Dropout [12], Drop-Conv2d [2], Weighted Channel Dropout [10], DropCluster [3], CorrDrop [26], LocalDrop [16], AutoDropout [19], etc. Our method, R-Block, is closely related to SpatialDropout and DropBlock. SpatialDropout randomly masks out entire channels of a feature map and DropBlock randomly drops square regions of a feature map. Since selecting contiguous blocks exploits the spatial correlation in feature maps, these two methods both have good regularization effects in CNNs. We design BDropDML and SDropDML by splitting channels and regions respectively to construct sub models with different dropping units. R-Block enforces the sub models to be consistent with each other to alleviate the training inconsistency. It is inspired by R-Drop [15] and generalizes the idea of "dropout twice" [5] from dropout to structured dropout variants. Our experiments show that R-Block is more effective than R-Drop in CNNs.

2 R-Block Regularization

This section introduces our proposed regularization method, R-Block, in detail. Given the training dataset $\mathcal{D} = \{(x, y)\}$, where $x \in \mathcal{R}^{m \times n \times c}$ and $y \in \{1, 2, 3, \dots, \kappa\}$ correspond to the image and its label in the dataset for the image classification task, $m \times n \times c$ is the height \times width \times channel dimension of a feature tensor and κ is the number of distinctive classes. The goal of the training is to learn a model F_Θ , where Θ represents all parameters in a CNN.

Given the input data (x, y) at each training step, we feed x to the forward pass of two sub models F_Θ^1 and F_Θ^2 with different drop regions. Therefore, we can obtain two distributions p_1 and p_2 of the model predictions, expressed as:

$$p_i^k(x) = \frac{\exp([F_\Theta^i(x)]_k/T)}{\sum_j \exp([F_\Theta^i(x)]_j/T)}, \quad (1)$$

where p_i^k represents the probability of the k th class for the i ($i = 1, 2$) sub model F_Θ^i , and $T > 0$ is the temperature scaling parameter.

The conventional supervised loss between the predicted values of the sub model F_Θ^i and the correct labels y is the standard cross-entropy loss J_{ce} :

$$J_{ce}(F_\Theta^i(x), y) = -\ln \frac{\exp([F_\Theta^i(x)]_y)}{\sum_j \exp([F_\Theta^i(x)]_j)}. \quad (2)$$

We use the Kullback Leibler (KL) Divergence to quantify the match of the output distributions p_1 and p_2 of two sub models. The KL distance J_{KL} from p_i and p_j is computed as:

$$J_{KL}(p_j, p_i) = \sum_k [p_j]_k \ln \frac{[p_j]_k}{[p_i]_k}. \quad (3)$$

The overall loss functions J_i for the sub model F_Θ^i is:

$$J_i(F_\Theta^i(x), y) = (1 - \alpha)J_{ce}(F_\Theta^i(x), y) + \alpha T^2 \sum_{j \neq i} J_{KL}(p_j, p_i), \quad (4)$$

where $\alpha > 0$ is the coefficient weight. Note that we multiply the square of the temperature T^2 by following the original KD [9].

The total training loss $J_{R-Block}$ is defined as follows:

$$J_{R-Block} = \frac{1}{|\mathcal{D}|} \sum_{(x,y) \in \mathcal{D}} \sum_i J_i(F_\Theta^i(x), y), \quad (5)$$

The overall framework of R-Block is shown in Figure 1.

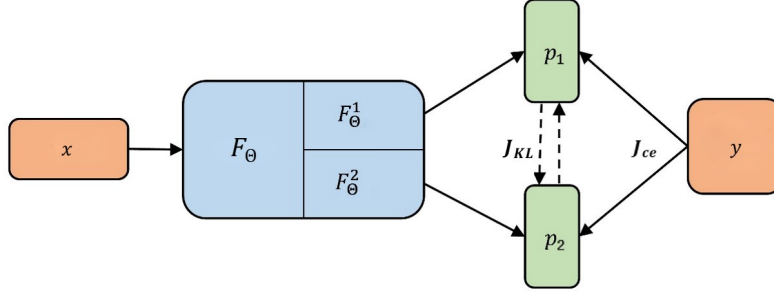


Figure 1: The overall framework of our proposed R-Block. The picture shows that one input x will go through two different sub models and obtain two distributions p_1 and p_2 . The total training loss includes the conventional supervised loss J_{ce} from correct labels and the KL Divergence J_{KL} between the two distributions of two sub models.

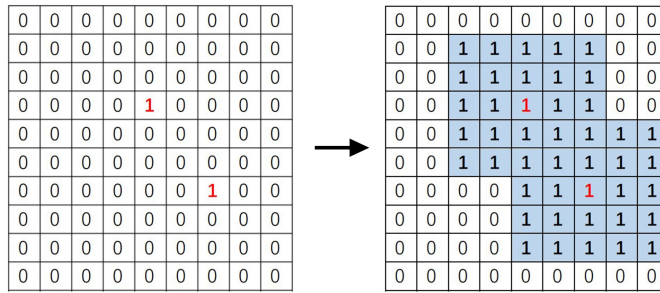


Figure 2: Example of mask sampling, where $b_{size} = 5$.

3 Sub models

In this section, we design two approaches, BDropDML and SDropDML, to construct sub models with completely different drop regions. There are two main parameters: b_{size} and p . b_{size} is the size of the block to be dropped, and p is the dropout probability for each activation unit.

We reference the mask sampling in DropBlock as shown in Figure 2: first, we compute the dropout probability γ of block center by the dropout probability p of each activation unit, and sample a mask M with probability γ on each feature map; second, every 1 entry on M is expanded to 1 block of $b_{size} \times b_{size}$. In order to position and maintain symmetry, b_{size} is usually set to an odd number. Here we denote $b_{size} = 2k + 1$.

3.1 BDropDML

We propose a strategy for constructing two sub models with complementary drop regions on feature channels, coined Block Dropout Deep Mutual Learning (BDropDML). Specifically, two sub models share the same DropBlock mask on each feature channel and then perform complementary mask division on channels with a probability of 0.5. The overall framework of BDropDML is shown in Figure 3, where the yellow Blocks represent drop regions.

Given one input $x \in \mathcal{R}^{m \times n \times c}$, the size b_{size} of the block to be dropped and the dropout probability p for each activation unit, the dropout probability γ of block center can be computed as:

$$\gamma = \frac{1}{b_{size}^2} p, \quad (6)$$

or:

$$\gamma = \frac{mn}{b_{size}^2 (m - b_{size} + 1)(n - b_{size} + 1)} p. \quad (7)$$

The details of BDropDML are given in Algorithm 1.

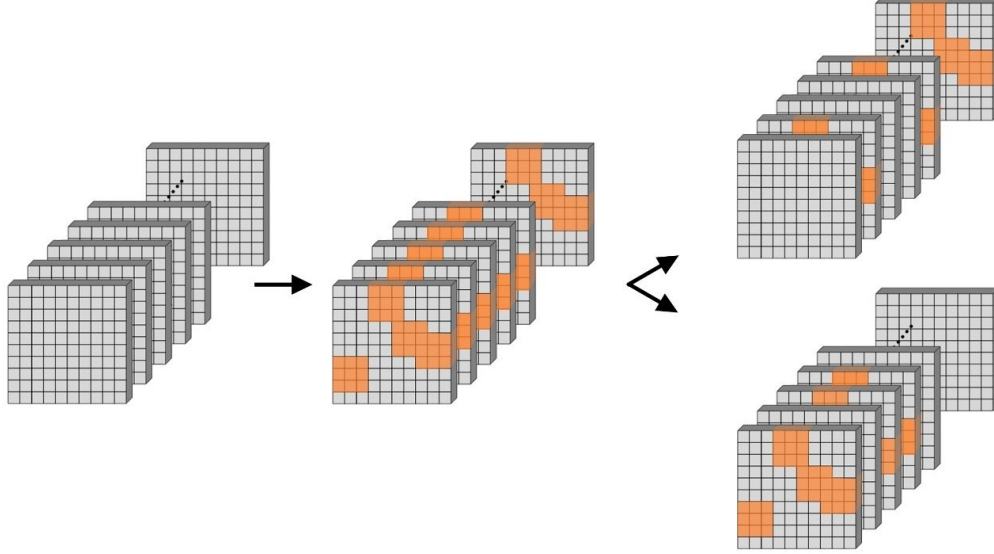


Figure 3: The overall framework of BDropDML.

Algorithm 1 BDropDML

Input: $x \in \mathcal{R}^{m \times n \times c}$, b_{size} , p .

Output: Masks sampling M^1 , M^2 .

- 1: Calculate γ by Eq. (6) or Eq. (7), randomly sample mask $r \in \mathcal{R}^{m \times n}$:
 $r_{i,j} \sim \text{Bernoulli}(1 - \gamma), \forall i \in \{1, 2, \dots, m\}, j \in \{1, 2, \dots, n\}$.
 - 2: For each 1 position $r_{i,j}$, create a spatial square mask $M \in \mathcal{R}^{m \times n}$ with the center being $r_{i,j}$, the width, height being b_{size} and set all the values of r in the square to be 1.
 - 3: Randomly sample mask $l^1 \in \mathcal{R}^c: l_k^1 \sim \text{Bernoulli}(0.5), \forall k \in \{1, 2, \dots, c\}$.
 Calculate $l^2 \in \mathcal{R}^c: l^2 = \mathbf{1}_{l^1} - l^1$.
 - 4: Expand M to $\hat{M} \in \mathcal{R}^{m \times n \times c}: \hat{M}_{i,j,k} = M_{i,j}$.
 Expand l^1, l^2 to $\hat{l}^1, \hat{l}^2 \in \mathcal{R}^{m \times n \times c}: \hat{l}_{i,j,k}^1 = l_k^1, \hat{l}_{i,j,k}^2 = l_k^2$,
 $\forall i \in \{1, 2, \dots, m\}, j \in \{1, 2, \dots, n\}, k \in \{1, 2, \dots, c\}$.
 - 5: Calculate: $\bar{M}^i = \mathbf{1}_x - \hat{M} \odot \hat{l}^i (i = 1, 2)$.
 - 6: Normalize the features: $M^i = \bar{M}^i / s^i$, where s^i is the proportion of 1 in $\bar{M}^i (i = 1, 2)$.
 - 7: Return M^1, M^2 .
-

3.2 SDropDML

We propose a strategy for constructing two sub models with complementary drop regions on the same channel, coined Spatial Dropout Deep Mutual Learning (SDropDML). Specifically, two sub models randomly drops the same channels of a feature map and then perform complementary DropBlock mask division with a probability of 0.5 on each dropped channel. The overall framework of SDropDML is shown in Figure 4, where the yellow Blocks represent drop regions.

When calculating the complementary DropBlock mask, we need to first estimate the dropout probability γ of block center based on the dropout probability $p = 0.5$. Given one input $x \in \mathcal{R}^{m \times n \times c}$ and the size $b_{size} = 2k + 1$, when $m, n > 2b_{size}$, the relationship between p and γ is as follows(detailed

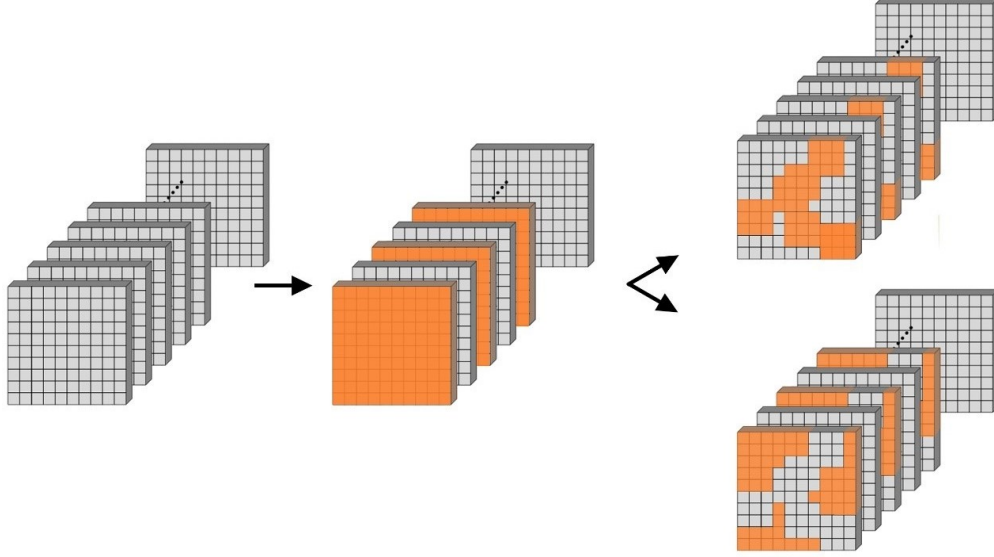


Figure 4: The overall framework of SDropDML.

proof can be found in Sec. 3.3):

$$\begin{aligned}
p &= \left(1 - \frac{2k}{m}\right)\left(1 - \frac{2k}{n}\right) \left(1 - (1 - \gamma)^{(2k+1)^2}\right) \\
&+ 4 \left[\frac{k^2}{mn} - \frac{1}{mn} \sum_{1 \leq i, j \leq k} (1 - \gamma)^{(k+i)(k+j)} \right] \\
&+ 2 \left(\frac{1}{m} + \frac{1}{n} - \frac{4k}{mn} \right) \left[k - (1 - \gamma)^{(2k+1)(k+1)} \frac{1 - (1 - \gamma)^{(2k+1)k}}{1 - (1 - \gamma)^{(2k+1)}} \right].
\end{aligned} \tag{8}$$

The details of SDropDML are given in Algorithm 2.

Algorithm 2 SDropDML

Input: $x \in \mathcal{R}^{m \times n \times c}$, b_{size} , p .

Output: Masks sampling M^1 , M^2 .

- 1: Randomly sample mask $l \in \mathcal{R}^c$: $l_k \sim \text{Bernoulli}(1 - p)$, $\forall k \in \{1, 2, \dots, c\}$.
 - 2: Estimate γ by Eq. (8) with $p = 0.5$, randomly sample mask $r \in \mathcal{R}^{m \times n}$:
 $r_{i,j} \sim \text{Bernoulli}(1 - \gamma)$, $\forall i \in \{1, 2, \dots, m\}, j \in \{1, 2, \dots, n\}$.
 - 3: For each 1 position $r_{i,j}$, create a spatial square mask $M^1 \in \mathcal{R}^{m \times n}$ with the center being $r_{i,j}$, the width, height being b_{size} and set all the values of r in the square to be 1.
Calculate $M^2 \in \mathcal{R}^{m \times n}$: $M^2 = \mathbf{1}_{M^1} - M^1$.
 - 4: Expand M^1, M^2 to $\hat{M}^1, \hat{M}^2 \in \mathcal{R}^{m \times n \times c}$: $\hat{M}_{i,j,k}^1 = M_{i,j}^1$, $\hat{M}_{i,j,k}^2 = M_{i,j}^2$.
Expand l to $\hat{l} \in \mathcal{R}^{m \times n \times c}$: $\hat{l}_{i,j,k} = l_k$,
 $\forall i \in \{1, 2, \dots, m\}, j \in \{1, 2, \dots, n\}, k \in \{1, 2, \dots, c\}$.
 - 5: Calculate: $\bar{M}^i = \mathbf{1}_x - \hat{l} \odot \hat{M}^i$ ($i = 1, 2$).
 - 6: Normalize the features: $M^i = \bar{M}^i / s^i$, where s^i is the proportion of 1 in \bar{M}^i ($i = 1, 2$).
 - 7: Return M^1, M^2 .
-

3.3 A the operational relationship between p and γ

In this section, we provide the derivation of Eq. 6 - 8 about the operational relationship between the dropout probability p of each activation unit and the dropout probability γ of block center.

Theorem 3.1. *Given one input $x \in \mathcal{R}^{m \times n \times c}$ and the size $b_{size} = 2k + 1$ of the block to be dropped, when $m, n > 2b_{size}$, the operational relationship between the dropout probability p of each activation unit and the dropout probability γ of block center can be described as:*

$$\begin{aligned} p &= \left(1 - \frac{2k}{m}\right)\left(1 - \frac{2k}{n}\right)\left(1 - (1 - \gamma)^{(2k+1)^2}\right) \\ &+ 4 \left[\frac{k^2}{mn} - \frac{1}{mn} \sum_{1 \leq i, j \leq k} (1 - \gamma)^{(k+i)(k+j)} \right] \\ &+ 2 \left(\frac{1}{m} + \frac{1}{n} - \frac{4k}{mn} \right) \left[k - (1 - \gamma)^{(2k+1)(k+1)} \frac{1 - (1 - \gamma)^{(2k+1)k}}{1 - (1 - \gamma)^{(2k+1)}} \right] \end{aligned}$$

Proof: Since the expansion principle of mask sampling in each channel is the same, we only consider the relationship between p and γ on $x \in \mathcal{R}^{m \times n}$.

Randomly sample mask $r \in \mathcal{R}^{m \times n}$: $r_{i,j} \sim \text{Bernoulli}(1 - \gamma)$. For each 1 position $r_{i,j}$, create a spatial square mask $M \in \mathcal{R}^{m \times n}$ with the center being $r_{i,j}$, the width, height being b_{size} and set all the values of r in the square to be 1.

Here, the dropout probability for each activation unit in M is p :

$$p([M]_{i,j} = 1 \mid 1 \leq i \leq m, 1 \leq j \leq n) = p, \quad (9)$$

We can calculate the expectation of the number of dropped activation units in M :

$$\mathbb{E} \left(\sum_{i,j} [M]_{i,j} \right) = \sum_{1 \leq i \leq m, 1 \leq j \leq n} p([M]_{i,j} = 1) = pmn, \quad (10)$$

In order to express the dropout probability of M with γ , we divide the mask M into 3 parts as shown in Figure 5.

In part I, the probability that the value of each activation unit equal to 1 can be expressed as:

$$\begin{aligned} &p([M]_{i,j} = 1 \mid k+1 \leq i \leq m-k, k+1 \leq j \leq n-k) \quad (11) \\ &= p \left(\max_{-k+1 \leq t, q \leq k+1} r_{i-1+t, j-1+q} = 1 \mid k+1 \leq i \leq m-k, k+1 \leq j \leq n-k \right) \\ &= 1 - p(r_{i-1+t, j-1+q} = 0 \mid \forall -k+1 \leq t, q \leq k+1) \\ &= 1 - (1 - \gamma)^{(2k+1)^2}. \end{aligned}$$

According to Eq.11, we have:

$$\begin{aligned} &\mathbb{E} \left(\sum_{i,j} [M]_{i,j} \mid [M]_{i,j} \in \text{I} \right) \quad (12) \\ &= \sum_{k+1 \leq i \leq m-k, k+1 \leq j \leq n-k} p([M]_{i,j} = 1) \\ &= \sum_{k+1 \leq i \leq m-k, k+1 \leq j \leq n-k} \left(1 - (1 - \gamma)^{(2k+1)^2} \right) \\ &= (m - 2k)(n - 2k) \left(1 - (1 - \gamma)^{(2k+1)^2} \right). \end{aligned}$$

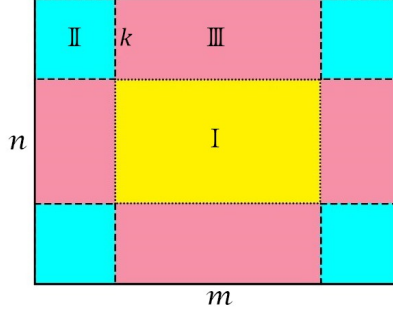


Figure 5: Partition of the mask $M \in \mathcal{R}^{m \times n}$.

In part II, due to symmetry, only the region $1 \leq i, j \leq k$ needs to be considered. Then we have:

$$\begin{aligned}
& p([M]_{i,j} = 1 \mid 1 \leq i, j \leq k) \\
&= p\left(\max_{-k+1 \leq t, q \leq k+1} r_{i-1+t, j-1+q} = 1 \mid 1 \leq i, j \leq k\right) \\
&= 1 - p(r_{i-1+t, j-1+q} = 0 \mid \forall 2-i \leq t \leq k+1, 2-j \leq q \leq k+1) \\
&= 1 - (1 - \gamma)^{(k+i)(k+j)}.
\end{aligned} \tag{13}$$

The expectation of the number of dropped activation units in part II can be calculated as:

$$\begin{aligned}
& \mathbb{E}\left(\sum_{i,j} [M]_{i,j} \mid [M]_{i,j} \in \text{II}\right) \\
&= 4 \sum_{1 \leq i, j \leq k} p([M]_{i,j} = 1) \\
&= 4 \sum_{1 \leq i, j \leq k} \left(1 - (1 - \gamma)^{(k+i)(k+j)}\right) \\
&= 4 \left[k^2 - \sum_{1 \leq i, j \leq k} (1 - \gamma)^{(k+i)(k+j)} \right].
\end{aligned} \tag{14}$$

In part III, due to symmetry, only the regions $k+1 \leq i \leq m-k$, $1 \leq j \leq k$ and $1 \leq i \leq k$, $k+1 \leq j \leq n-k$ needs to be considered. The probability that the value of each activation unit in the regions $k+1 \leq i \leq m-k$, $1 \leq j \leq k$ equal to 1 can be expressed as:

$$\begin{aligned}
& p([M]_{i,j} = 1 \mid k+1 \leq i \leq m-k, 1 \leq j \leq k) \\
&= p\left(\max_{-k+1 \leq t, q \leq k+1} r_{i-1+t, j-1+q} = 1 \mid k+1 \leq i \leq m-k, 1 \leq j \leq k\right) \\
&= 1 - p(r_{i-1+t, j-1+q} = 0 \mid \forall -k+1 \leq t \leq k+1, 2-j \leq q \leq k+1) \\
&= 1 - (1 - \gamma)^{(2k+1)(k+j)}.
\end{aligned} \tag{15}$$

According to Eq 15, we have:

$$\begin{aligned}
& \mathbb{E} \left(\sum_{i,j} [M]_{i,j} \mid k+1 \leq i \leq m-k, 1 \leq j \leq k \right) \\
&= \sum_{k+1 \leq i \leq m-k, 1 \leq j \leq k} p([M]_{i,j} = 1) \\
&= \sum_{k+1 \leq i \leq m-k, 1 \leq j \leq k} \left(1 - (1-\gamma)^{(2k+1)(k+j)} \right) \\
&= (m-2k) \sum_{1 \leq j \leq k} \left(1 - (1-\gamma)^{(2k+1)(k+j)} \right) \\
&= (m-2k) \left[k - (1-\gamma)^{(2k+1)(k+1)} \frac{1 - (1-\gamma)^{(2k+1)k}}{1 - (1-\gamma)^{(2k+1)}} \right].
\end{aligned}$$

In the same way, the probability that the value of each activation unit in the regions $1 \leq i \leq k$, $k+1 \leq j \leq n-k$ equal to 1 can be expressed as:

$$\begin{aligned}
& p([M]_{i,j} = 1 \mid 1 \leq i \leq k, k+1 \leq j \leq n-k) \tag{16} \\
&= p \left(\max_{-k+1 \leq t, q \leq k+1} r_{i-1+t, j-1+q} = 1 \mid 1 \leq i \leq k, k+1 \leq j \leq n-k \right) \\
&= 1 - p(r_{i-1+t, j-1+q} = 0 \mid \forall 2-i \leq t \leq k+1, -k+1 \leq q \leq k+1) \\
&= 1 - (1-\gamma)^{(k+i)(2k+1)}.
\end{aligned}$$

The corresponding expectation can be calculated as:

$$\begin{aligned}
& \mathbb{E} \left(\sum_{i,j} [M]_{i,j} \mid 1 \leq i \leq k, k+1 \leq j \leq n-k \right) \\
&= \sum_{1 \leq i \leq k, k+1 \leq j \leq n-k} p([M]_{i,j} = 1) \\
&= \sum_{1 \leq i \leq k, k+1 \leq j \leq n-k} \left(1 - (1-\gamma)^{(k+i)(2k+1)} \right) \\
&= (n-2k) \left[k - (1-\gamma)^{(2k+1)(k+1)} \frac{1 - (1-\gamma)^{(2k+1)k}}{1 - (1-\gamma)^{(2k+1)}} \right].
\end{aligned}$$

The expectation of the number of dropped activation units in part III can be calculated as:

$$\begin{aligned}
& \mathbb{E} \left(\sum_{i,j} [M]_{i,j} \mid [M]_{i,j} \in \text{III} \right) \tag{17} \\
&= 2\mathbb{E} \left(\sum_{i,j} [M]_{i,j} \mid k+1 \leq i \leq m-k, 1 \leq j \leq k \right) \\
&+ 2\mathbb{E} \left(\sum_{i,j} [M]_{i,j} \mid 1 \leq i \leq k, k+1 \leq j \leq n-k \right) \\
&= 2(m+n-4k) \left[k - (1-\gamma)^{(2k+1)(k+1)} \frac{1 - (1-\gamma)^{(2k+1)k}}{1 - (1-\gamma)^{(2k+1)}} \right].
\end{aligned}$$

Combined with Eq. 10, Eq. 12, Eq. 14 and Eq. 17, we have:

$$\begin{aligned}
pmn &= (m - 2k)(n - 2k) \left(1 - (1 - \gamma)^{(2k+1)^2}\right) \\
&+ 4 \left[k^2 - \sum_{1 \leq i, j \leq k} (1 - \gamma)^{(k+i)(k+j)} \right] \\
&+ 2(m + n - 4k) \left[k - (1 - \gamma)^{(2k+1)(k+1)} \frac{1 - (1 - \gamma)^{(2k+1)k}}{1 - (1 - \gamma)^{(2k+1)}} \right].
\end{aligned}$$

Divided by mn , we can get the result. \square

Particularly, when we use a sample mask r to generate a spatial square mask M without considering marginal loss, we have:

$$p = 1 - (1 - \gamma)^{b_{size}^2}. \quad (18)$$

If we only sample mask r in part III in Figure 5, we have:

$$pmn = (m - b_{size} + 1)(n - b_{size} + 1) \left(1 - (1 - \gamma)^{b_{size}^2}\right),$$

that is:

$$p = \frac{(m - b_{size} + 1)(n - b_{size} + 1) \left(1 - (1 - \gamma)^{b_{size}^2}\right)}{mn}. \quad (19)$$

For the same γ , we denote the probabilities calculated by Eq. 18 and Eq. 19 as p_1 and p_1 respectively, and then p obtained by Eq. 8 satisfies:

$$p_2 \leq p \leq p_1. \quad (20)$$

Suppose the value of γ is small, according to the McLoughlin expansion, we have:

$$1 - (1 - \gamma)^{b_{size}^2} \sim b_{size}^2 \gamma. \quad (21)$$

Combined with Eq. 18 and Eq. 19, we can easily get Eq. 6 and Eq. 7.

In addition, we need to estimate γ by Eq. 8 with $p = 0.5$ in Algorithm 2. In fact, γ increases monotonously with the increase of p from 0 to 1. Here, we calculate the initial values of γ through Eq. 6 and Eq. 7 with $p = 0.5$ and then adjustment γ according to Eq. 8 and Monotonicity Eq. 20.

4 Experiments

4.1 Experimental setup

Datasets. We demonstrate the effectiveness of R-Block on various image classification datasets: CIFAR-10, CIFAR-100 [13] and TinyImageNet [4]. The CIFAR-10 and CIFAR-100 datasets consist of 32×32 color images containing objects from 10 and 100 classes respectively. Both are split into a 50,000-image train set and a 10,000-image test set. The TinyImageNet dataset contains 120,000 64×64 colour images of 200 object classes.

Network architecture. We demonstrate our method on ResNet-18, ResNet-34 [7] and VGG16 [20]. We modify the first convolutional layer of ResNet-18 with kernel size 3×3 , strides 1 and padding 1, instead of the kernel size 7×7 , strides 2 and padding 3 [8].

Implementation Details. We use stochastic gradient descents (SGD) with a momentum of 0.9, an initial rate of 0.1, weight decay of $5e - 4$ and batch size of 128. The learning rate is decayed by the factor of 0.1 at 75, 130 and 180 epochs for all datasets. The total epoch is set as 200, the temperature T is 3 and the coefficient weight α is 0.1. We set the dropout probability parameter p as 0.2 and the block size b_{size} as 3. Since baselines are usually overfitted for the longer training scheme and have lower validation accuracy at the end of training, we report the highest validation accuracy over the full training course for fair comparison.

Model	Method	p	CIFAR-10	CIFAR-100
ResNet-18	Baseline	0	92.98	71.28
	Dropout	0.5	92.71	70.47
	SpatialDropout	0.1	93.02	71.30
	DropBlock	0.1	93.02	71.38
	R-Block(BDropDML)	0.2	93.49	72.35
	R-Block(SDropDML)	0.2	93.56	72.08
VGG16	Baseline	0	93.64	73.20
	Dropout	0.5	93.56	72.93
	SpatialDropout	0.1	93.75	73.08
	DropBlock	0.1	93.71	73.27
	R-Block(BDropDML)	0.2	94.24	73.80
	R-Block(SDropDML)	0.2	94.21	73.98

Table 1: Top-1 (%) accuracy on the CIFAR datasets and different model architectures. The best and second-best results are indicated in black bold and blue bold respectively.

Method	p	TinyImageNet
Baseline	0	42.96
SpatialDropout	0-0.1	43.02
DropBlock	0-0.1	43.07
R-Block(BDropDML)	0-0.2	43.37
R-Block(SDropDML)	0-0.2	43.35

Table 2: Top-1 (%) accuracy on the TinyImageNet dataset and ResNet-34. The best and second-best results are indicated in black bold and blue bold respectively. In this experiments, we use a linear scheme of increasing the value of dropout probability. This linear scheme is similar to ScheduledDropPath [30].

4.2 Classification accuracy

We measure the top-1 (%) accuracy of R-Block by comparing with Dropout, SpatialDropout and DropBlock on various datasets and model architectures. The results are presented in Table 1 and Table 2. These results imply that R-Block induces better classification performance than others. For example, R-Block(BDropDML) improves the top-1 (%) accuracy of Baseline from 71.28% to 72.35% under the CIFAR-100 dataset and ResNet-18. We also observe that the top-1 (%) accuracy of Dropout with greater dropout probability tends to be worse than Baseline, which perhaps caused by insufficient training due to too many dropped activation unit.

4.3 Methods with different sub models

We provide six approaches to construct sub models as shown in Figure 6 (a)-(f). The details of these approaches are listed below:

- (a) This approach is to use Dropout in fully connected layers twice randomly, corresponding to R-Drop [15].
- (b) This approach is inspired by R-Drop and two sub models have complementary drop regions in fully connected layers. We denote it as C-Drop.
- (c) This approach is to use SpatialDropout twice randomly and we denote it as R-SpatialDropout.
- (d) This approach is to use DropBlock twice randomly and we denote it as R-DropBlock.
- (e) This approach is BDropDML in Sec. 3.1, corresponding to ours method R-Block(BDropDML).
- (f) This approach is SDropDML in Sec. 3.2, corresponding to ours method R-Block(SDropDML).

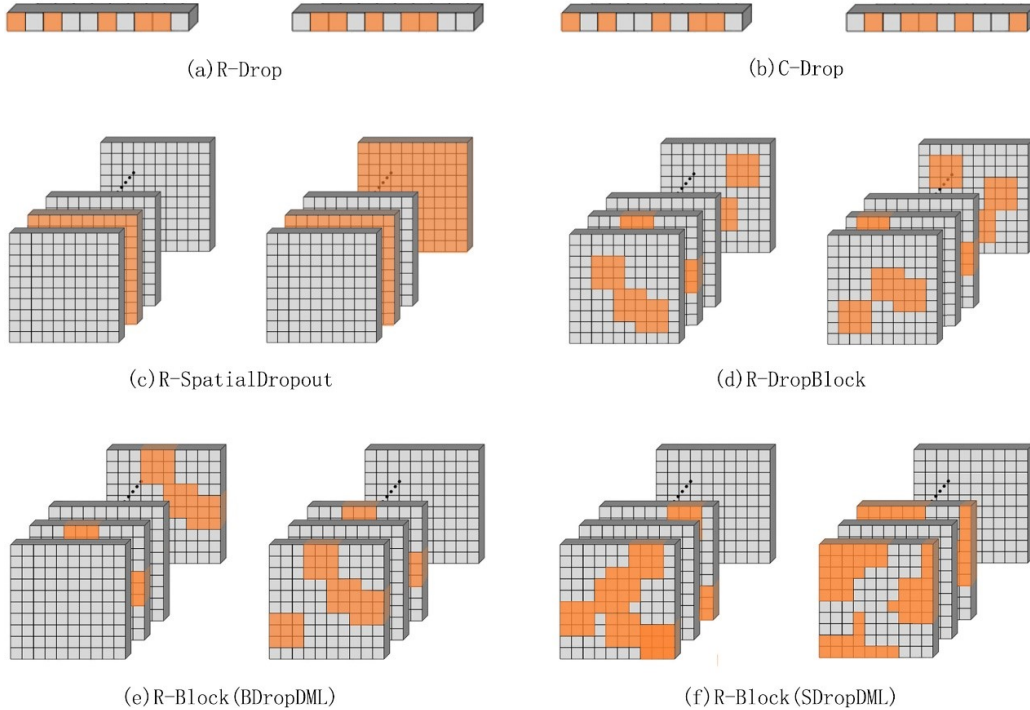


Figure 6: Different approaches to construct sub models.

Method	p	Training stages				
		20%	40%	60%	80%	100%
R-Drop	0.5	54.93	68.88	68.99	70.81	71.17
C-Drop	0.5	54.60	69.50	69.70	71.03	71.30
R-SpatialDropout	0.1	55.80	69.83	69.98	71.41	71.86
R-DropBlock	0.1	56.20	69.81	70.30	71.15	71.60
R-Block(BDropDML)	0.2	56.83	70.21	70.83	71.98	72.35
R-Block(SDropDML)	0.2	58.19	70.15	70.31	71.49	72.08

Table 3: Top-1 (%) accuracy of various methods with different sub models at different training stages on CIFAR-100 and ResNet-18. Each stage adopts the optimal model of the current stage. The best and second-best results are indicated in black bold and blue bold respectively.

We report the performance of R-Drop, C-Drop, R-SpatialDropout, R-DropBlock, R-Block(BDropDML) and R-Block(SDropDML) corresponding to (a)-(f) respectively at different training stages in Table 3. The results show that our R-Block performs the best. These also show that methods using sub models with different drop regions outperform methods using sub models with random drop regions. Sub models with complementary drop regions enable each activation unit to update during training. At the same time, since the drop regions of two sub models in BDropDML and SDropDML are completely different, the difference in semantic information of the feature map is extracted to the greatest extent, which greatly improves the regularization efficiency of the sub models.

5 Conclusion and Future Work

In this paper, we propose R-Block to regularize training CNNs. R-Block is a form of structured dropout and can reduce the inconsistency of the model structure between training and inference phases by minimizing the mutual learning losses on the outputs of two sub models for each data sample in training. We introduce BDropDML and SDropDML to construct sub models with different

drop regions. Our experiments on CIFAR and TinyImageNet demonstrate that R-Block performs better than other existing structured dropout variants and methods using sub models with different drop regions outperform methods using sub models with random drop regions. Our next step is to consider adding an attention mechanism on feature maps and dynamically segment the drop regions to construct sub models more reasonably.

References

- [1] Jimmy Ba, Jamie Ryan Kiros, and Geoffrey E. Hinton. Layer normalization. *ArXiv*, abs/1607.06450, 2016.
- [2] Shaofeng Cai, Jinyang Gao, Meihui Zhang, Wei Wang, Gang Chen, and Beng Chin Ooi. Effective and efficient dropout for deep convolutional neural networks. *ArXiv*, abs/1904.03392, 2019.
- [3] Liyang Chen, Philip Gautier, and Sergül Aydıre. Dropcluster: A structured dropout for convolutional networks. *ArXiv*, abs/2002.02997, 2020.
- [4] Jia Deng, Wei Dong, Richard Socher, Li-Jia Li, K. Li, and Li Fei-Fei. Imagenet: A large-scale hierarchical image database. *2009 IEEE Conference on Computer Vision and Pattern Recognition*, pp. 248–255, 2009.
- [5] Tianyu Gao, Xingcheng Yao, and Danqi Chen. Simcse: Simple contrastive learning of sentence embeddings. *ArXiv*, abs/2104.08821, 2021.
- [6] Golnaz Ghiasi, Tsung-Yi Lin, and Quoc V. Le. Dropblock: A regularization method for convolutional networks. In *Neural Information Processing Systems*, 2018.
- [7] Kaiming He, X. Zhang, Shaoqing Ren, and Jian Sun. Deep residual learning for image recognition. *2016 IEEE Conference on Computer Vision and Pattern Recognition (CVPR)*, pp. 770–778, 2016.
- [8] Kaiming He, X. Zhang, Shaoqing Ren, and Jian Sun. Identity mappings in deep residual networks. In *European Conference on Computer Vision*, 2016.
- [9] Geoffrey E. Hinton, Oriol Vinyals, and Jeffrey Dean. Distilling the knowledge in a neural network. *ArXiv*, abs/1503.02531, 2015.
- [10] Saihui Hou and Zilei Wang. Weighted channel dropout for regularization of deep convolutional neural network. In *AAAI Conference on Artificial Intelligence*, 2019.
- [11] Sergey Ioffe and Christian Szegedy. Batch normalization: Accelerating deep network training by reducing internal covariate shift. In *International Conference on Machine Learning*, 2015.
- [12] Salman Hameed Khan, Munawar Hayat, and Fatih Murat Porikli. Regularization of deep neural networks with spectral dropout. *Neural networks : the official journal of the International Neural Network Society*, 110:82–90, 2017.
- [13] Alex Krizhevsky. Learning multiple layers of features from tiny images. 2009.
- [14] Yang D. Li, Weizhi Ma, C. Chen, M. Zhang, Yiqun Liu, Shaoping Ma, and Yue Yang. A survey on dropout methods and experimental verification in recommendation. *IEEE Transactions on Knowledge and Data Engineering*, 35:6595–6615, 2022.
- [15] Xiaobo Liang, Lijun Wu, Juntao Li, Yue Wang, Qi Meng, Tao Qin, Wei Chen, M. Zhang, and Tie-Yan Liu. R-drop: Regularized dropout for neural networks. *ArXiv*, abs/2106.14448, 2021.
- [16] Ziqing Lu, Chang Xu, Bo Du, Takashi Ishida, L. Zhang, and Masashi Sugiyama. Localdrop: A hybrid regularization for deep neural networks. *IEEE Transactions on Pattern Analysis and Machine Intelligence*, 44:3590–3601, 2021.
- [17] Xuezhe Ma, Yingkai Gao, Zhiting Hu, Yaoliang Yu, Yuntian Deng, and Eduard H. Hovy. Dropout with expectation-linear regularization. *ArXiv*, abs/1609.08017, 2016.

- [18] Sungeon Park and Nojun Kwak. Analysis on the dropout effect in convolutional neural networks. In *Asian Conference on Computer Vision*, 2016.
- [19] Hieu Pham and Quoc V. Le. Autodropout: Learning dropout patterns to regularize deep networks. In *AAAI Conference on Artificial Intelligence*, 2021.
- [20] Karen Simonyan and Andrew Zisserman. Very deep convolutional networks for large-scale image recognition. *CoRR*, abs/1409.1556, 2014.
- [21] Nitish Srivastava, Geoffrey E. Hinton, Alex Krizhevsky, Ilya Sutskever, and Ruslan Salakhutdinov. Dropout: a simple way to prevent neural networks from overfitting. *J. Mach. Learn. Res.*, 15:1929–1958, 2014.
- [22] Christian Szegedy, Vincent Vanhoucke, Sergey Ioffe, Jon Shlens, and Zbigniew Wojna. Rethinking the inception architecture for computer vision. In *Proceedings of the IEEE conference on computer vision and pattern recognition*, pp. 2818–2826, 2016.
- [23] Jonathan Tompson, Ross Goroshin, Arjun Jain, Yann LeCun, and Christoph Bregler. Efficient object localization using convolutional networks. *2015 IEEE Conference on Computer Vision and Pattern Recognition (CVPR)*, pp. 648–656, 2015.
- [24] Haibing Wu and Xiaodong Gu. Towards dropout training for convolutional neural networks. *Neural networks : the official journal of the International Neural Network Society*, 71:1–10, 2015.
- [25] Yuxin Wu and Kaiming He. Group normalization. In *Proceedings of the European conference on computer vision (ECCV)*, pp. 3–19, 2018.
- [26] Yuyuan Zeng, Tao Dai, Bin Chen, Shutao Xia, and Jian Lu. Correlation-based structural dropout for convolutional neural networks. *Pattern Recognit.*, 120:108117, 2021.
- [27] Linfeng Zhang, Jiebo Song, Anni Gao, Jingwei Chen, Chenglong Bao, and Kaisheng Ma. Be your own teacher: Improve the performance of convolutional neural networks via self distillation. In *Proceedings of the IEEE/CVF International Conference on Computer Vision*, pp. 3713–3722, 2019.
- [28] Ying Zhang, Tao Xiang, Timothy M Hospedales, and Huchuan Lu. Deep mutual learning. In *Proceedings of the IEEE Conference on Computer Vision and Pattern Recognition*, pp. 4320–4328, 2018.
- [29] Konrad Zolna, Devansh Arpit, Dendi Suhubdy, and Yoshua Bengio. Fraternal dropout. *ArXiv*, abs/1711.00066, 2017.
- [30] Barret Zoph, Vijay Vasudevan, Jonathon Shlens, and Quoc V. Le. Learning transferable architectures for scalable image recognition. *2018 IEEE/CVF Conference on Computer Vision and Pattern Recognition*, pp. 8697–8710, 2017.